Radiation Measurements 177 (2024) 107264

Contents lists available at ScienceDirect

Radiation Measurements

journal homepage: www.elsevier.com/locate/radmeas

Calculation of relative luminescent efficiency of TL/OSL detectors to cosmic radiation spectrum in cis-lunar space

P. Bilski [a,*], D. Matthiä [b], T. Berger [b], R. Gaza [c,d]

[a] Institute of Nuclear Physics, Polish Academy of Sciences, IFJ PAN, PL-31-342, Krakow, Poland
[b] Institute of Aerospace Medicine, German Aerospace Center, DLR, 51147, Cologne, Germany
[c] Leidos, Space Exploration and Mission Operations, Houston, USA
[d] Space Radiation Analysis Group, NASA Johnson Space Center, Houston, USA

ABSTRACT

In the MARE experiment onboard the NASA Artemis 1 mission of the ORION spacecraft to lunar orbit, two anthropomorphic female phantoms, equipped with a large number of active and passive radiation detectors were flown. Among the detectors were both LiF:Mg,Ti and LiF:Mg,Cu,P TL detectors as well as Al_2O_3:C OSL detectors. In order to correctly interpret the measured doses, the effective relative TL/OSL efficiency for cosmic radiation of these detectors was calculated by combining simulated radiation spectra for the cis-lunar space conditions with the efficiency functions based on experimental data for different ions and on a microdosimetric model.

The obtained results show that for the ORION shielding conditions, the relative efficiency of LiF:Mg,Ti is close to unity (0.95), while the remaining detectors show somewhat smaller efficiency: 0.90 for Al_2O_3:C and (0.81–0.86) for LiF:Mg,Cu,P. The analysis of the influence of the shielding thickness on the relative TL/OSL efficiency revealed, that for low shielding conditions, the relative efficiency may be more significantly decreased, reaching values between 0.71 (LiF:Mg,Cu,P) and 0.85 (LiF:Mg,Ti) for 1 g/cm^2.

1. Introduction

Passive luminescent detectors are frequently used for dosimetry of cosmic radiation during spaceflights (Berger et al., 2013, 2016; Bilski, 2018). The cosmic radiation spectrum is extremely complex, consisting of a great variety of particles with energy and linear energy transfer (LET) values extending over many orders of magnitude. This complexity of the spectrum may have a significant impact on the results measured by thermally (TL) and optically (OSL) stimulated detectors, as their relative detection efficiency is known to depend on the ionization density (Berger and Hajek, 2008; Bilski et al., 2011).

The relative TL/OSL efficiency is usually defined as the luminescent signal per unit dose for a given radiation type, divided by the same quantity for the reference gamma radiation (usually used for calibration of detectors):

$$\eta = (I/D)_k \, / (I/D)_\gamma$$

where: η - relative efficiency, I – intensity of the signal, D – absorbed dose, k – radiation type. If the relative efficiency is less than unity (i.e., for $\eta < 1$), the doses measured using the gamma calibration are underestimated. Over the last two decades, much effort has been devoted to investigating the relative TL/OSL efficiency for energetic ions by exploiting the HIMAC accelerator and other facilities (Berger et al., 2006; Bilski, 2006; De Saint-Hubert et al., 2021; Gaza et al., 2004; Olko and Bilski, 2021; Parisi et al., 2017; Sądel et al., 2016; Teichmann et al., 2018; Uchihori et al., 2002; Yasuda et al., 2006; Yukihara et al., 2004, 2006, 2022), enabling gathering of a huge amount of good quality experimental data on TL/OSL efficiency for different ions.

With this collected data, an attempt could be made to calculate the effective TL efficiency to cosmic radiation by folding the experimental efficiency values with the simulated cosmic radiation spectrum for the low Earth orbit conditions (Bilski et al., 2016). These calculations were performed so far for LiF:Mg,Ti and LiF:Mg,Cu,P TL detectors. The main conclusion was that LiF:Mg,Ti has a relative efficiency within a few percent of unity, while LiF:Mg,Cu,P underestimates cosmic radiation doses by more than 15%. The high effective efficiency of LiF:Mg,Ti despite the observed decreased response for heavy ions, was found to be due to the high efficiency to the protons trapped in the Earth radiation belt. From this, it was concluded that for interplanetary missions the TL efficiency might be lower, due to the absence of the trapped proton component.

On November 16, 2022 the NASA Artemis 1 flight of the ORION spacecraft to the Moon orbit was launched. One of the secondary

* Corresponding author.
E-mail address: pawel.bilski@ifj.edu.pl (P. Bilski).

https://doi.org/10.1016/j.radmeas.2024.107264
Received 13 June 2024; Received in revised form 26 July 2024; Accepted 1 August 2024
Available online 2 August 2024

scientific payloads of this mission was the Matroshka AstroRad Experiment (MARE), consisting of the exposure of two anthropomorphic female phantoms, equipped with a large number of active and passive radiation detectors (Berger, 2023). Among the detectors were both LiF:Mg,Ti and LiF:Mg,Cu,P, as well as Al_2O_3:C OSL detectors. In order to correctly interpret the measured doses, it was necessary to perform an analysis similar to that previously performed for low Earth orbit, but for the radiation spectrum present in cis-lunar space and this was the motivation of the current work.

In addition, since the previous publication, a new microdosimetric model of TL/OSL efficiency has been developed and published (Parisi, 2018; Parisi et al., 2018b, 2019, 2020b, 2020a, 2022), which describes the efficiency for the most important components of the cosmic radiation spectrum. In our earlier work, the relative efficiency to ions was based on empirical fits to the experimental data. The available data covered only a limited range of energies and a limited number of ion species (although the main hydrogen data were quite abundant), so it was necessary to apply some simplifications. Now, the microdosimetric model covers a much wider range of the radiation spectrum, making the obtained results more reliable.

2. Calculation of cosmic radiation spectrum in cis-lunar space

The radiation field from galactic cosmic rays (GCR) in cis-lunar space behind shielding was calculated using the same methodology as in (Bilski et al., 2016). GCRs form the omni present ionizing radiation field in space, that varies in intensity during the solar cycle and that consists mostly of fully ionized nuclei (Reitz, 2008). Taking into account their respective abundances and biological effects, hydrogen to iron, sometimes nickel, in the energy range from approximately 10-100 MeV/nucleon to 200 GeV/nucleon are considered relevant for radiation protection purposes. GCRs can penetrate thick shielding and create a complex field of primary and secondary particles through interactions with the shielding material. The primary radiation source was ions from hydrogen to nickel using the galactic cosmic ray model from (Matthiä et al., 2013) and using Oulu Neutron Monitor count rates in November 2022 to derive the model parameter W = 43.5 for the GCR intensity. The primary particles were transported through the shielding geometry with the Geant4 version 11.00 Monte-Carlo toolkit (Agostinelli et al., 2003; Allison et al., 2006, 2016) using the physics list QGSP_INCLXX_HP_EMZ. The shielding geometry consisted of a spherical shell of aluminium with an inner radius of 2 m and either a uniform thickness corresponding to 1, 15, 30, 60, 100 or 200 g/cm^2 or a variable thickness derived from a ray-tracing of the ORION module using solid angle fractions calculated from the cumulative distribution function (see (Bilski et al., 2016) for a detailed description of the procedure). Differential particle energy spectra were calculated inside the aluminium shielding and converted to LET spectra in a post-processing procedure using pre-calculated tables (all LET values used in this paper represent unrestricted LET in water). These tables were separately calculated with Geant4 for particles normally incident on a 0.3 mm water layer and contain the energy deposition distribution per particle and energy for all particles under consideration. The LET spectra were then calculated as the sum over all particle energies of the energy deposition distributions scaled by the number of particles at the given energy and normalized by the layer thickness. The energy spectra and the derived LET spectra inside the different shielding geometries were calculated for protons, electrons/positrons, photons (gammas), muons, pions, and ions from helium to iron. Neutron spectra were calculated as well but not used in the further efficiency analysis of the TL/OSL detectors (since there is not enough data to model TL/OSL efficiency for neutrons).

Dose spectra were also calculated from the LET spectra through multiplication of the particle fluence rate with the LET; the results for the ORION shielding are illustrated in Figs. 1–3. The dose below approximately 0.6 keV/μm is dominated by protons, electrons, and positrons. Helium nuclei start contributing above this value, which approximately equals the most probable energy deposition per pathlength for minimum-ionizing alpha particles and which is slightly below the average energy deposition per pathlength of minimum ionizing alpha particle of 0.8 keV/μm; protons are the single most important contribution up to 10–20 keV/μm, above which heavier nuclei dominate.

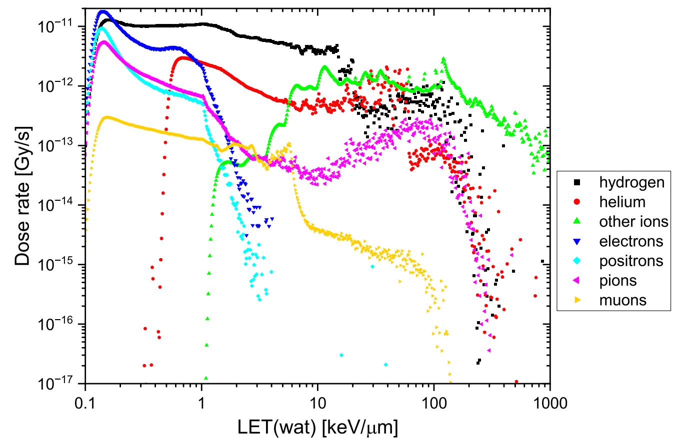

Fig. 1. Calculated dose spectra of the different components of the cosmic radiation field inside the ORION shielding.

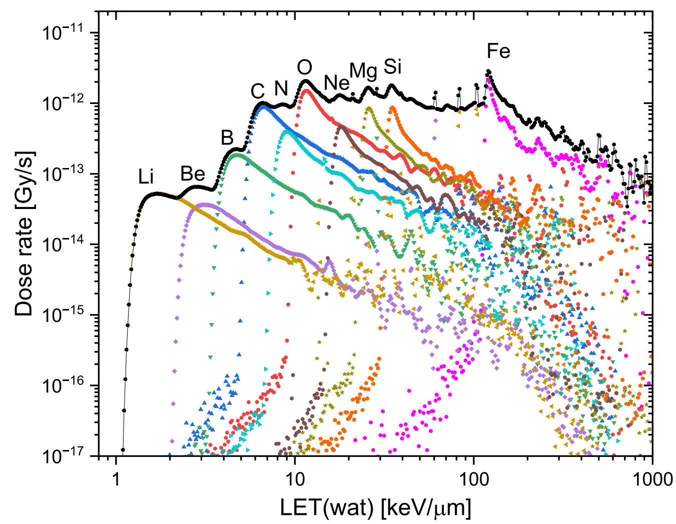

Fig. 2. Calculated dose spectra of ions with Z > 2 inside the ORION shielding. Black symbols – total spectrum, coloured symbols – ions with the major contributions to the spectrum.

3. Relative TL/OSL efficiency for components of the cosmic radiation spectrum

While in the last decades a lot of experimental data on the relative efficiency of TL/OSL detectors to energetic ions was gathered, they still cannot fully cover the whole spectrum of cosmic radiation. In recent years Parisi developed a microdosimetric model of luminescent efficiency, which covers a broader part of the cosmic radiation spectrum (Parisi, 2018; Parisi et al., 2018a, 2018b, 2019). For that reason, this work was based on the model data published by Parisi (Parisi, 2018; Parisi et al., 2020b, 2022) for TL of LiF:Mg,Ti and LiF:Mg,Cu,P, as well as OSL (blue emission) of Al_2O_3:C. The available data included the following ions: H, He, Li, C, O, Ne, Si, Ar and Fe (no Li data for Al_2O_3:C). For the remaining relevant ions, the efficiency values were obtained by interpolation. The results are presented in Figs. 4–6.

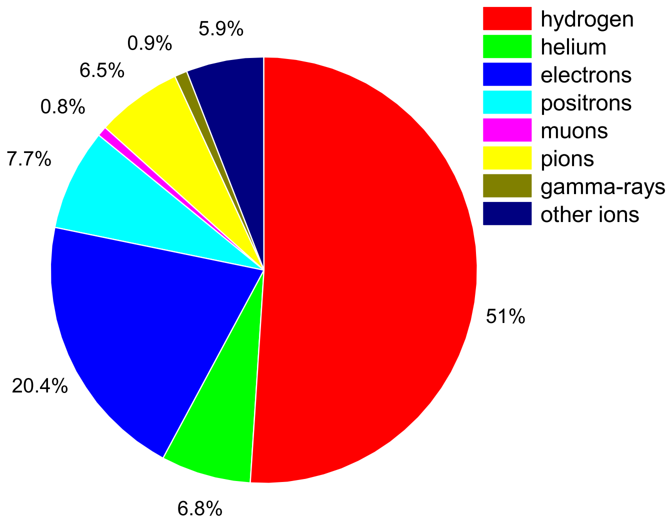

Fig. 3. Calculated relative contributions of the different components of the cosmic radiation spectrum to the dose inside the ORION shielding (without neutrons). Hydrogen and helium include deuteron, Triton and ^{3}He, respectively.

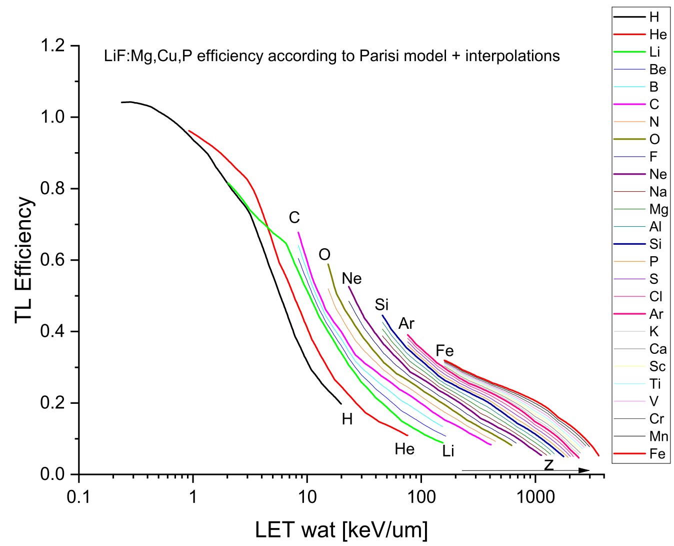

Fig. 5. Relative TL efficiency of LiF:Mg,Cu,P according to the Parisi model (Parisi, 2018). Arrow indicates increasing atomic number Z.

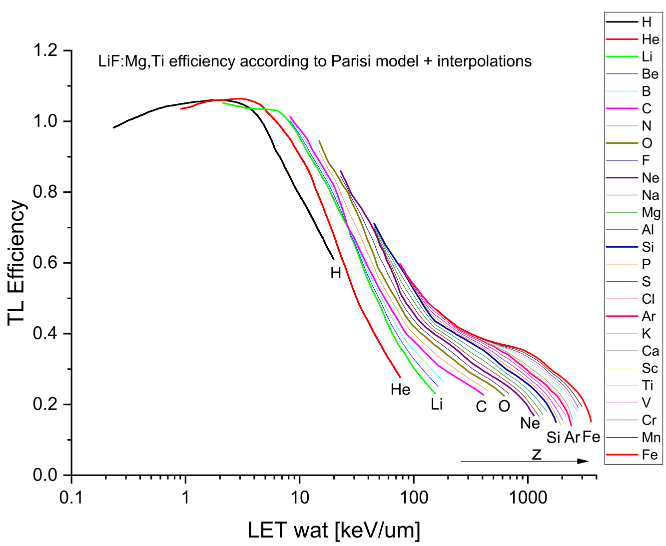

Fig. 4. Relative TL efficiency of LiF:Mg,Ti according to the Parisi model (Parisi, 2018). Arrow indicates increasing atomic number Z.

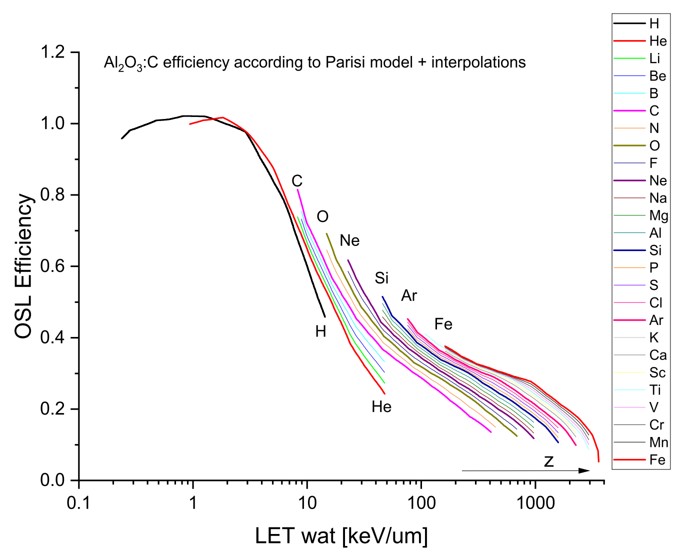

Fig. 6. Relative OSL efficiency of Al_2O_3:C according to the Parisi model (Parisi et al., 2022). Arrow indicates increasing atomic number Z.

For the low-LET region, where no data are available, a constant efficiency was assumed, equal to the last available data point. An exception is protons, which are the main component of the cosmic ray spectrum and also have a larger number of efficiency data available, so they were analysed separately.

In the case of LiF:Mg,Ti efficiency for protons (Fig. 7) there are some differences between the available experimental data and the microdosimetric model, especially above about 5 keV/μm. It should be however noted that experimental data for low-energy protons, whose range is comparable with a typical TLD thickness, might be biased by higher uncertainties. The model also predicts a somewhat smaller overresponse for 2–3 MeV protons. It is not possible to decide which data are more reliable, therefore, further calculations were performed with both the microdosimetric model of Parisi and the function fitted to the experimental data (the same function as used in (Bilski et al., 2016)).

In the case of LiF:Mg,Cu,P (Fig. 8), the differences between the microdosimetric model and the fitted function used in the previous calculations appear to be more significant, as the model systematically predicts higher efficiency values. It was speculated that this overestimation of LiF:Mg,Cu,P efficiency for protons may be caused by an instability of the low-temperature peak of the TL glow curve (charge transfer to the main peak) (Parisi et al., 2019). Further calculations were again carried out for both microdosimetric model and the fitted function. For Al_2O_3:C only the microdosimetric model values were used, without any modifications.

It should be noted that the microdosimetric model was developed relying on a particular set of experimental data, which were obtained using the particular experimental protocol. The model possesses one free parameter (so-called ‘target size’), which value was chosen by Parisi et al. to obtain the best agreement between the model and the experimental efficiency data (target sizes of 40 nm for both LiF TLDs and 100 nm for Al_2O_3:C were used) (Parisi et al., 2018b, 2019, 2022). Using other experimental protocols may lead to deviation between the model and experimental results.

The space radiation spectrum consists not only of ions but also of lighter particles such as electrons, muons, and pions, that are created through interactions of the primary cosmic radiation with mass

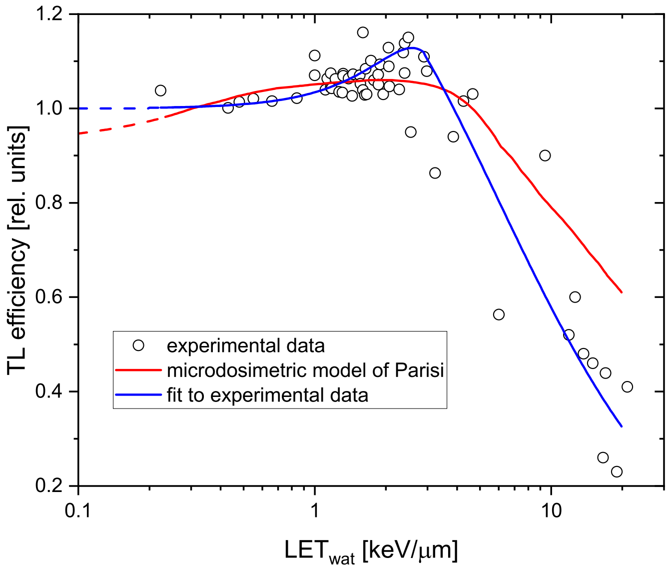

Fig. 7. LiF:Mg,Ti TL efficiency for protons. Experimental data points represent the dataset compiled from various experiments in (Olko and Bilski, 2021), supplemented by the data for 0.223 keV/μm (1 GeV) (Bilski, 2005). Broken lines represent extrapolation below the range of available data.

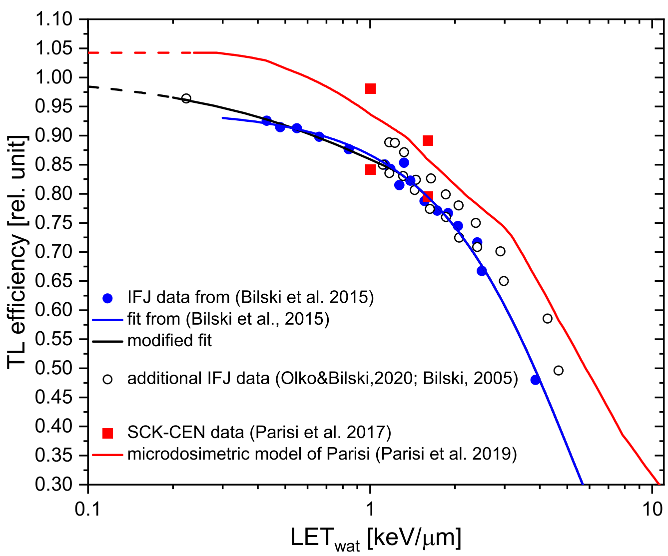

Fig. 8. LiF:Mg,Cu,P TL efficiency for protons. Comparison between IFJ data (with the corresponding fitted function) used in the previous calculations of TL efficiency to cosmic radiation, with additional IFJ data (with the modified fit), data from (Parisi et al., 2017) and microdosimetric model of Parisi (Parisi et al., 2019).

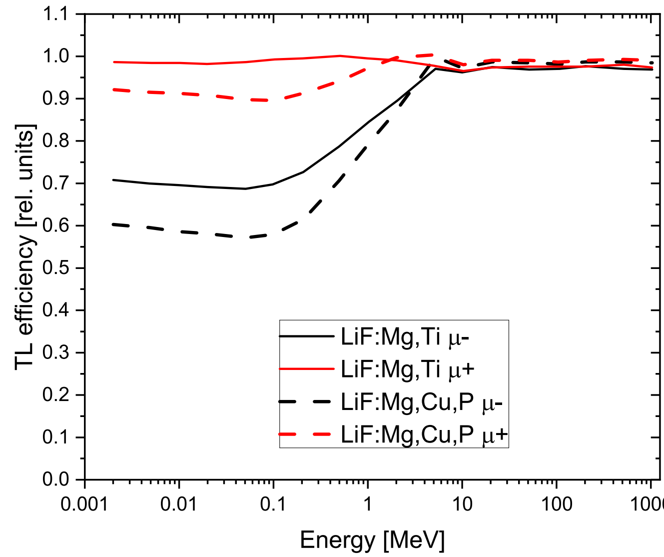

Fig. 9. Relative TL efficiency of LiF:Mg,Ti and LiF:Mg,Cu,P for muons according to the microdosimetric model (Parisi et al., 2020b).

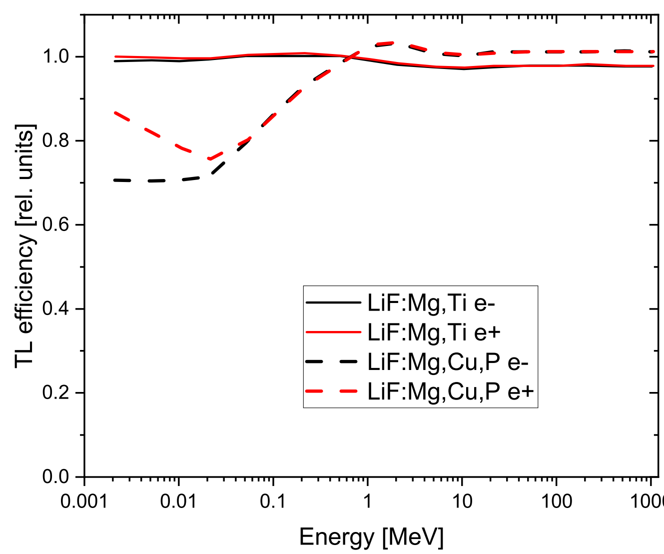

Fig. 10. Relative TL efficiency of LiF:Mg,Ti and LiF:Mg,Cu,P for electrons and positrons according to the microdosimetric model (Parisi et al., 2020a).

shielding. There is very little experimental data on the efficiency of TLDs/OSLDs for these particles. In the case of LiF-based detectors, calculations are available according to the microdosimetric model (Parisi et al., 2020a, 2020b). Figs. 9–11 show the TL efficiencies extracted from these publications as a function of particle energy. For further calculations, the energy values were converted into stopping power using the data shown in Fig. 12. The values of the stopping power were obtained from tabulated data in Geant4 for the collision stopping power due to ionization in water (using the G4EmCalculator class, for details see Geant4 "Book for Application Developers", https://geant4.web.cern.ch/docs/). In the case of Al_2O_3:C no model data have been published. In order to enable a complete calculation of space radiation efficiency also for this material, a rough estimate of the efficiency to electrons, muons, pions was attempted based on the relation to LiF detectors. Most of the cosmic ray dose spectra of electrons, muons, and pions lies below 1 keV/μm and very little above 10 keV/μm. This range of LET is covered by the lightest ions, i.e., hydrogen and helium. The ratio of the relative OSL efficiency of Al_2O_3:C for these ions to that of LiF:Mg,Ti is presented in Fig. 13. The relative efficiency of Al_2O_3:C for the lighter particles was then approximated by multiplying corresponding values for LiF:Mg,Ti by the values of a function fitted to the data from Fig. 13.

Finally, for gamma-rays relative efficiency equal to unity was assumed for all detector types.

4. Results - calculation of the effective TL/OSL efficiency to cosmic radiation spectrum

The effective (or average) TL/OSL efficiency η for cosmic radiation spectrum was calculated using the following formula:

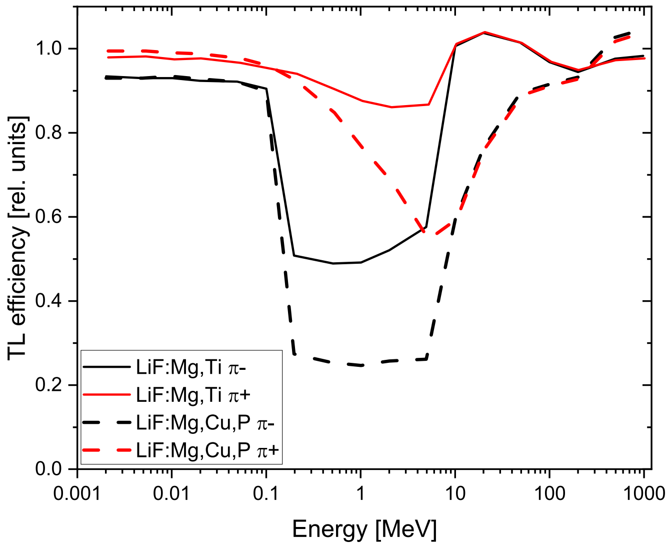

Fig. 11. Relative TL efficiency of LiF:Mg,Ti and LiF:Mg,Cu,P for pions according to the microdosimetric model (Parisi et al., 2020b).

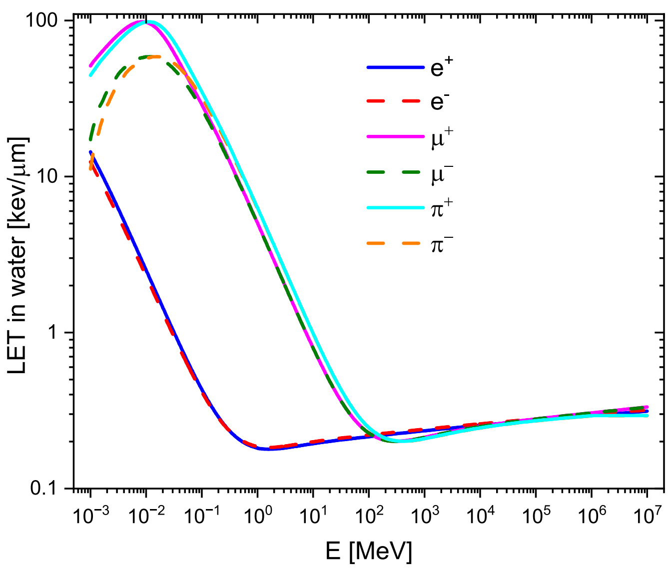

Fig. 12. Relationship between LET in water and energy for electrons, muons, and pions.

$$\eta = \frac{\sum_{Z=1}^{26}\sum_{L}\eta_Z(L)D_Z(L) + \sum_i\sum_{L}\eta_i(L)D_i(L)}{\sum_{Z=1}^{26}\sum_{L}D_Z(L) + \sum_i\sum_{L}D_i(L)}$$

where L – LET in water, Z – atomic number of the considered ions, $i \in$(e−, e+, π-, π+, μ-, μ+, γ), D*(L)* - doses of different components of the studied spectrum (calculated as described in section 2 and shown in Figs. 1 and 2), $\eta(L)$ – relative efficiency for particular particles (calculated as described in section 3).

For LiF:Mg,Ti the analyses were carried out for both efficiency functions shown in Fig. 7: microdosimetric model and fit to the experimental data. The calculations produced effective efficiencies η of 0.953 and 0.943, respectively. In addition, two boundary cases were considered: upper boundary - taking the higher value of two models for each LET value, and lower boundary - taking the lower values. This calculation gave η values of 0.960 and 0.936 respectively. The spread of the obtained values is very small, with a mean of 0.948. It appears,

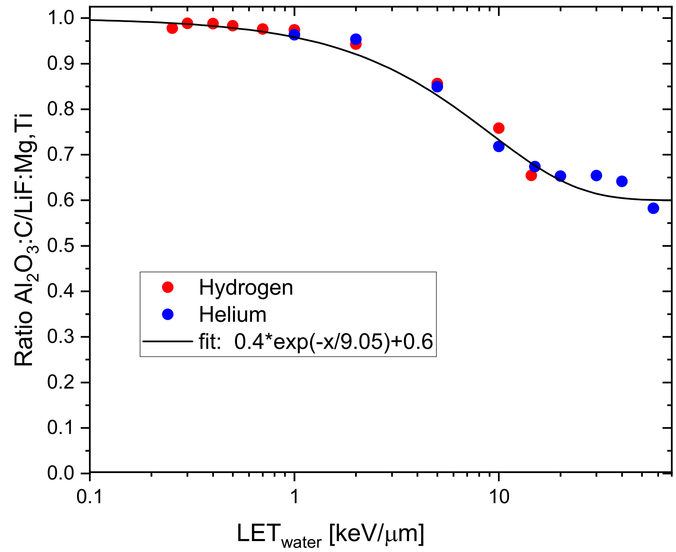

Fig. 13. Ratio of the relative efficiencies of Al_2O_3:C and LiF:Mg,Ti for protons and helium ions, as calculated according to the microdosimetric model.

therefore, that the apparent differences between the approaches have a small effect on the effective efficiency.

In the case of LiF:Mg,Cu,P the calculations using two considered models (see Fig. 8) produced somewhat more different values of the effective efficiency: 0.860 for the microdosimetric model and 0.807 for the empirical fit to the data. As there is no ground to point out which one of these values is more accurate, in further analysis both of them were included. In the case of Al_2O_3:C no variants of the model were considered and η equal to 0.897 was obtained.

The estimation of the uncertanties of the calculated luminescent eficency to cosmic radiation spectrum is not straightforward. Parisi provided only a general assessment of the deviation between the microdosimetric model and the experimental data used for its development, which were below 10% in the great majority of cases (Parisi, 2018; Parisi et al., 2022). Another indication of the range of the uncertainties of the whole approach may be obtained from the differences between η values calculated for protons using the microdosimetric model and the purely empirical fit to the experimental data. The largest difference of 6.5% was obtained for LiF:Mg,Cu,P and it seems reasonable to assume, that the maximum possible error should not be much higher than that. The accuracy of the TL efficiency models for protons is probably the largest contributor to the uncertainties in the calculated efficiencies, as protons deliver over 50% of the total dose. The next most important component of the spectrum is electrons/positrons, but for these particles the relative efficiency is mostly close to unity, so the influence of the possible uncertainty on the overall results should not be large. Uncertainties in the relative efficiency for pions, calculated entirely on the basis of the microdosimetric model without any confirmation by the experimental data, may be of some importance. However, since pions contribute only about 6% of the dose, even if the model values are substantially incorrect, the contribution to the uncertainties in the overall efficiency should not be larger than 1–2%. Finally, it should be noted that the uncertainties for Al_2O_3:C might be larger, mainly due to the aforementioned lack of the microdosimetric model for particles other than ions, as well as due to the more scarce experimental data.

Fig. 14 presents the contributions provided by the individual particles to the relative TL/OSL efficiency. The differences between detector types are rather small. In all of the detectors about half of the signal is calculated to be due to protons and about 20% due to electrons, in general agreement with the contribution of these particles to the total dose.

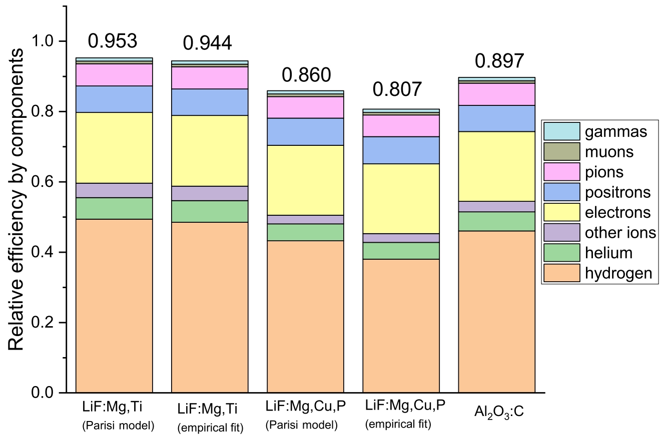

Fig. 14. Contributions of different components of the radiation field to the relative TL/OSL efficiency of the studied detectors.

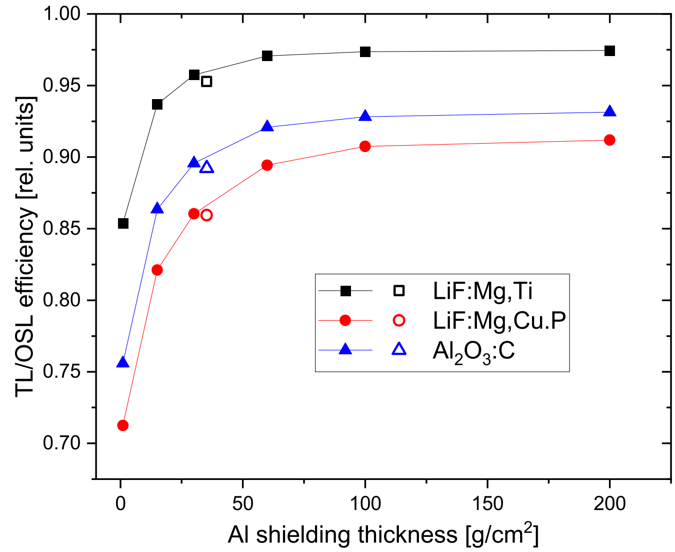

Fig. 16. Dependence of the relative TL/OSL efficency for cis-lunar radiation spectrum on Al shielding thickness (full symbols and lines). Open symbols - relative TL/OSL efficency calculated for the spectrum inside the ORION shielding (median shielding thickness of 35.2 g/cm^2 was assumed). Neutrons have not been considered.

More differences are revealed if one examines which particles are responsible for the decreased (quenched) effciency. Breakdown by component of the effective relative efficiency deficit, defined as the difference (1-η), is shown in Fig. 15. For LiF:Mg,Cu,P most of the effciency deficit is due to protons, while for LiF:Mg,Ti heavier ions have more impact concerning efficiency quenching. This is due to the fact, that efficiency is exceeding unity in a certain proton energy range of LiF:Mg,Ti (see Fig. 7).

The calculated values of the relative efficiency for the MARE experiment are very similar to those obtained in the previous work for the Earth orbit, which for the conditions of the Columbus module of the ISS amounted to about 0.97 for LiF:Mg,Ti and 0.83 for LiF:Mg,Cu,P (Bilski et al., 2016). It may appear at first sight a somewhat surprising result, as it was expected that for the deep space conditions, the efficiency would be decreased in comparison with the low Earth orbit due to the absence of the trapped protons and the increased relative contribution of heavier ions. The lack of a substanial decrease may be however explained by examining the influence of the shielding thickness on the relative TL efficiency. Such a relationship was previousely studied for the galactic cosmic rays at the low Earth orbit (Bilski et al., 2016). Fig. 16 presents the results obtained for the cis-lunar radiation spectrum. It can be seen that for low shielding the relative efficiency of all detectors is indeed much decreased, but with increasing shielding thickness it is rapidly growing, reaching a pleateau at c.a. 50 g/cm^2. For the shielding thickness of 25 g/cm^2 the η for LiF:Mg,Ti excceds 0.95. The modelled median shielding of the ORION is 35.2 g/cm^2, so efficiency values are close to the maximum levels.

Fig. 17 shows the contributions of different components of the radiation spectrum to the dose as a function of the shielding thickness. These data help to explain the observed increase of the relative TL/OSL efficiency in the first 50 g/cm^2 of the shielding thickness. This effect is caused by the steep decrease of the contribution of helium and heavier ions to the dose.

5. Conclusions

The effective relative TL/OSL efficiency for cosmic radiation of three detector types used in the MARE experiment was calculated by combining simulated spectra for the cis-lunar space conditions with the

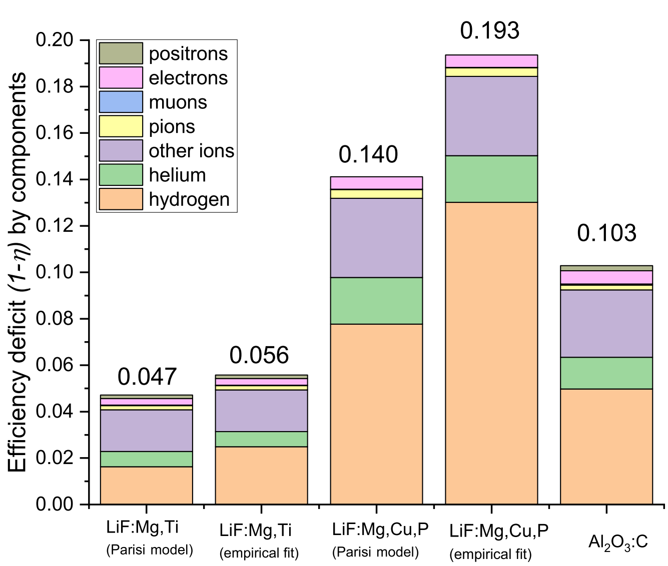

Fig. 15. Breakdown by component of the effective relative efficiency deficit (1-η).

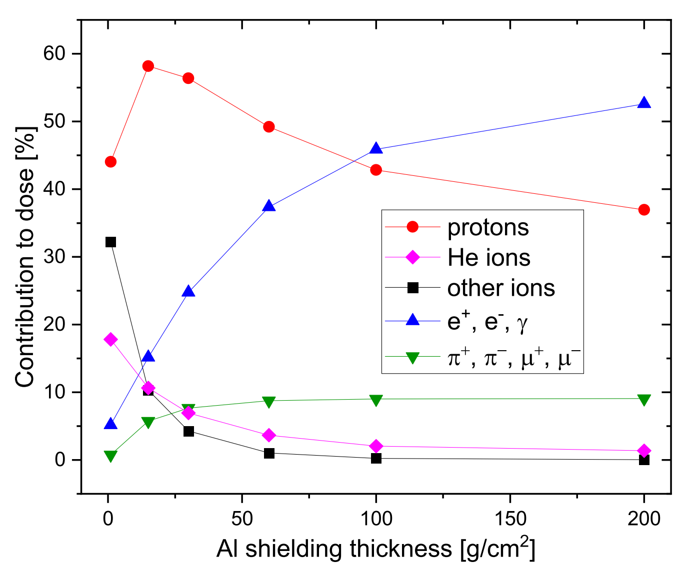

Fig. 17. Contributions of different components of the radiation spectrum at cis-lunar space to the dose vs. shielding thickness.

efficiency functions based on experimental data for different ions and on the microdosimetric model. For the radiation spectrum inside the ORION shielding TL efficiency of LiF:Mg,Ti was found to be equal to about 0.95. This means, that the results obtained with this most standard TL detector type may be considered as correct (within a few percent uncertainties) also for such radiation spectra. The remaining detectors show somewhat more decreased efficiency: 0. 90 for Al_2O_3:C and (0.81–0.86) for LiF:Mg,Cu,P.

The analysis of the influence of the shielding thickness on the relative TL/OSL efficiency revealed, that for low shielding conditions, the relative efficiency may be more significantly decreased, reaching values between 0.71 (LiF:Mg,Cu,P) and 0.85 (LiF:Mg,Ti) for 1 g/cm^2. This effect is caused by the more pronounced presence of densely ionizing helium and heavier ions, which amounts to about 50% of the dose for this shielding thickness, in contrast to just a few percent for the ORION conditions under which most heavier ions have fragmented into lighter elements or stopped. The possibility of underestimated results should therefore be taken into account, if measurements in low shielding conditions were to be carried out.

CRediT authorship contribution statement

P. Bilski: Writing – original draft, Methodology, Investigation, Funding acquisition, Conceptualization. **D. Matthiä:** Writing – review & editing, Software, Investigation. **T. Berger:** Writing – review & editing, Supervision, Investigation. **R. Gaza:** Writing – review & editing, Validation, Resources.

Declaration of competing interest

The authors declare that they have no known competing financial interests or personal relationships that could have appeared to influence the work reported in this paper.

Data availability

Data will be made available on request.

Acknowledgments

This work was funded by the National Science Centre, Poland (grant No 2020/39/B/ST9/00459). DLR was funded for this work by "FuW Strahlenrisiken ME 2475075".

The authors would like to thank the Sodankyla Geophysical Observatory and the website team (http://cosmicrays.oulu.fi) for providing the Oulu neutron monitor data used to derive the GCR model parameter.

References

Agostinelli, S., Allison, J., Amako, K., et al., 2003. Geant4—a simulation toolkit. Nucl. Instrum. Methods A 506, 250–303. https://doi.org/10.1016/S0168-9002(03)01368-8.

Allison, J., Amako, K., Apostolakis, J., et al., 2006. Geant4 developments and applications. IEEE Trans. Nucl. Sci. 53, 270–278. https://doi.org/10.1109/TNS.2006.869826.

Allison, J., Amako, K., Apostolakis, J., et al., 2016. Recent developments in Geant4. Nucl. Instrum. Methods A 835, 186–225. https://doi.org/10.1016/j.nima.2016.06.125.

Berger, T., 2023. NASA Artemis I mission and the MARE experiment. In: 26th Workshop on Radiation Monitoring for International Space Station (WRMISS), Rome, Italy. https://wrmiss.org/workshops/twentysixth/.

Berger, T., Bilski, P., Hajek, M., Puchalska, M., Reitz, G., 2013. The MATROSHKA experiment: results and comparison from EVA (MTR-1) and IVA (MTR-2A/2B) exposure. Radiat. Res. 180, 622–637. https://doi.org/10.1667/RR13148.1.

Berger, T., Hajek, M., 2008. TL-efficiency - overview and experimental results over the years. Radiat. Meas. 43, 146–156. https://doi.org/10.1016/j.radmeas.2007.10.029.

Berger, T., Hajek, M., Summerer, L., Fugger, M., Vana, N., 2006. The efficiency of various thermoluminescence dosemeter types to heavy ions. Radiat. Protect. Dosim. 120, 365. https://doi.org/10.1093/rpd/nci582.

Berger, T., Przybyla, B., Matthiä, D., et al., 2016. DOSIS & DOSIS 3D: long-term dose monitoring onboard the Columbus laboratory of the international space station (ISS). J. Space Weather Space Clim. 6, A39. https://doi.org/10.1051/swsc/2016034.

Bilski, P., 2005. Characterisation of TLDs used within the MATROSHKA project – results of ICCHIBAN-6 and NSRL-ICCHIBAN experiments. In: 10th Workshop on Radiation Monitoring for International Space Station (WRMISS), Chiba, Japan. https://wrmiss.org/workshops/tenth/.

Bilski, P., 2006. Response of various LiF thermoluminescent detectors to high energy ions - results of the ICCHIBAN experiment. Nucl. Instrum. Methods Phys. Res. B 251, 121–126. https://doi.org/10.1016/j.nimb.2006.05.012.

Bilski, P., 2018. Thermoluminescent dosimetry of cosmic radiation in space. In: Chen, R., Pagonis, V. (Eds.), Advances in Physics and Applications of Optically and Thermally Stimulated Luminescence. World Scientific, pp. 285–317. https://doi.org/10.1142/9781786345790_0008.

Bilski, P., Berger, T., Hajek, M., Reitz, G., 2011. Comparison of the response of various TLDs to cosmic radiation and ion beams: current results of the HAMLET project. Radiat. Meas. 46, 1680–1685. https://doi.org/10.1016/j.radmeas.2011.03.023.

Bilski, P., Matthiä, D., Berger, T., 2016. Influence of cosmic radiation spectrum and its variation on the relative efficiency of LiF thermoluminescent detectors – calculations and measurements. Radiat. Meas. 88, 33–40. https://doi.org/10.1016/j.radmeas.2016.02.029.

De Saint-Hubert, M., Castellano, F., Leblans, P., Sterckx, P., Kodaira, S., Swakoń, J., de Freitas Nascimento, L., 2021. Characterization of 2D Al_2O_3:C,Mg radiophotoluminescence films in charged particle beams. Radiat. Meas. 141, 106518 https://doi.org/10.1016/j.radmeas.2021.106518.

Gaza, R., Yukihara, E.G., McKeever, S.W.S., 2004. The response of thermally and optically stimulated luminescence from Al_2O_3:C to high-energy heavy charged particles. Radiat. Meas. 38, 417–420. https://doi.org/10.1016/j.radmeas.2003.12.027.

Matthiä, D., Berger, T., Mrigakshi, A.I., Reitz, G., 2013. A ready-to-use galactic cosmic ray model. Adv. Space Res. 51, 329–338. https://doi.org/10.1016/j.asr.2012.09.022.

Olko, P., Bilski, P., 2021. Microdosimetric understanding of dose response and relative efficiency of thermoluminescence detectors. Radiat. Protect. Dosim. https://doi.org/10.1093/rpd/ncaa211.

Parisi, A., 2018. Space and Hadron Therapy with Luminescent Detectors: Microdosimetric Modeling and Experimental Measurements. PhD Thesis. Polytech of Mons.

Parisi, A., Sawakuchi, G., Granville, D., Yukihara, E.G., 2022. Microdosimetric modeling of the relative efficiency of Al_2O_3:C (Luxel, blue emission) optically stimulated luminescent detectors exposed to ions from ^{1}H to ^{132}Xe. Radiat. Meas. 150, 106678 https://doi.org/10.1016/j.radmeas.2021.106678.

Parisi, A., Struelens, L., Vanhavere, F., 2020a. Nanoscale calculation of the relative efficiency of ^{7}LiF:Mg,Ti (MTS-7) and ^{7}LiF:Mg,Cu,P (MCP-7) thermoluminescent detectors for measuring electrons and positrons. J. Phys.: Conf. Series 1662, 012025. https://doi.org/10.1088/1742-6596/1662/1/012025.

Parisi, A., Struelens, L., Vanhavere, F., 2020b. The relative efficiency of ^{7}LiF:Mg,Ti (MTS-7) and ^{7}LiF:Mg,Cu,P (MCP-7) thermoluminescent detectors for muons, pions and kaons over a broad energy range (2 keV–1 GeV): theoretical calculations using the Microdosimetric d(z) Model. Radiat. Phys. Chem. 177, 109096 https://doi.org/10.1016/j.radphyschem.2020.109096.

Parisi, A., Van Hoey, O., Megret, P., Vanhavere, F., 2017. The influence of the dose assessment method on the LET dependence of the relative luminescence efficiency of LiF:Mg, Ti and LiF:Mg, Cu. P. Radiat. Meas. 98, 34. https://doi.org/10.1016/j.radmeas.2017.02.001.

Parisi, A., Van Hoey, O., Megret, P., Vanhavere, F., 2018a. Microdosimetric specific energy probability distribution in nanometric targets and its correlation with the efficiency of thermoluminescent detectors exposed to charged particles. Radiat. Meas. 123, 1. https://doi.org/10.1016/j.radmeas.2018.12.010.

Parisi, A., Van Hoey, O., Megret, P., Vanhavere, F., 2019. Microdosimetric modeling of the relative luminescence efficiency of LiF:Mg,Cu,P (MCP) detectors exposed to charged particles. Radiat. Protect. Dosim. 183, 172–176. https://doi.org/10.1093/rpd/ncy272.

Parisi, A., Van Hoey, O., Vanhavere, F., 2018b. Microdosimetric modeling of the relative luminescence efficiency of LiF:Mg,Ti (MTS) detectors exposed to charged particles. Radiat. Protect. Dosim. 180, 192–195. https://doi.org/10.1093/rpd/ncx188.

Reitz, G., 2008. Characteristic of the radiation field in low earth orbit and in deep space. Zeitschrift fur Medizinische Physik 18, 233–243. https://doi.org/10.1016/j.zemedi.2008.06.015.

Sądel, M., Bilski, P., Swakoń, J., Weber, A., 2016. Evaluation of the relative TL efficiency of the thermoluminescent detectors to heavy charged particles. Radiat. Protect. Dosim. 168, 27–32. https://10.1093/rpd/ncv003.

Teichmann, T., Gonzales Torres, M.J., van Goethem, M.J., et al., 2018. Dose and dose rate measurements in proton beams using the luminescence of beryllium oxide. J. Instrum. 13, P10015. https://10.1088/1748-0221/13/10/P10015.

Uchihori, Y., Fujitaka, K., Yasuda, N., Benton, E., 2002. Intercomparison of radiation instruments for cosmic-ray with heavy ion beams at NIRS (ICCHIBAN project). J. Radiat. Res. 43, S81–S85. https://doi.org/10.1269/jrr.43.S81.

Yasuda, N., Uchihori, Y., Benton, E.R., Kitamura, H., Fujitaka, K., 2006. The intercomparison of cosmic rays with heavy ion beams at NIRS (ICCHIBAN) project. Radiat. Protect. Dosim. 120, 414–420. https://doi.org/10.1093/rpd/nci536.

Yukihara, E.G., Christensen, J.B., Togno, M., 2022. Demonstration of an optically stimulated luminescence (OSL) material with reduced quenching for proton therapy dosimetry: MgB_4O_7:Ce,Li. Radiat. Meas. 152, 106721 https://doi.org/10.1016/j.radmeas.2022.106721.

Yukihara, E.G., Gaza, R., McKeever, S.W.S., Soares, C.G., 2004. Optically stimulated luminescence and thermoluminescence efficiencies for high-energy heavy charged particle irradiation in Al_2O_3:C. Radiat. Meas. 38, 59–70. https://doi.org/10.1016/S1350-4487(03)00251-8.

Yukihara, E.G., Sawakuchi, G.O., Guduru, S., McKeever, S.W.S., Gaza, R., Benton, E.R., Yasuda, N., Uchihori, Y., Kitamura, H., 2006. Application of the optically stimulated luminescence (OSL) technique in space dosimetry. Radiat. Meas. 41, 1126–1135. https://doi.org/10.1016/j.radmeas.2006.05.027.